SUPPLEMENTAL MATERIAL

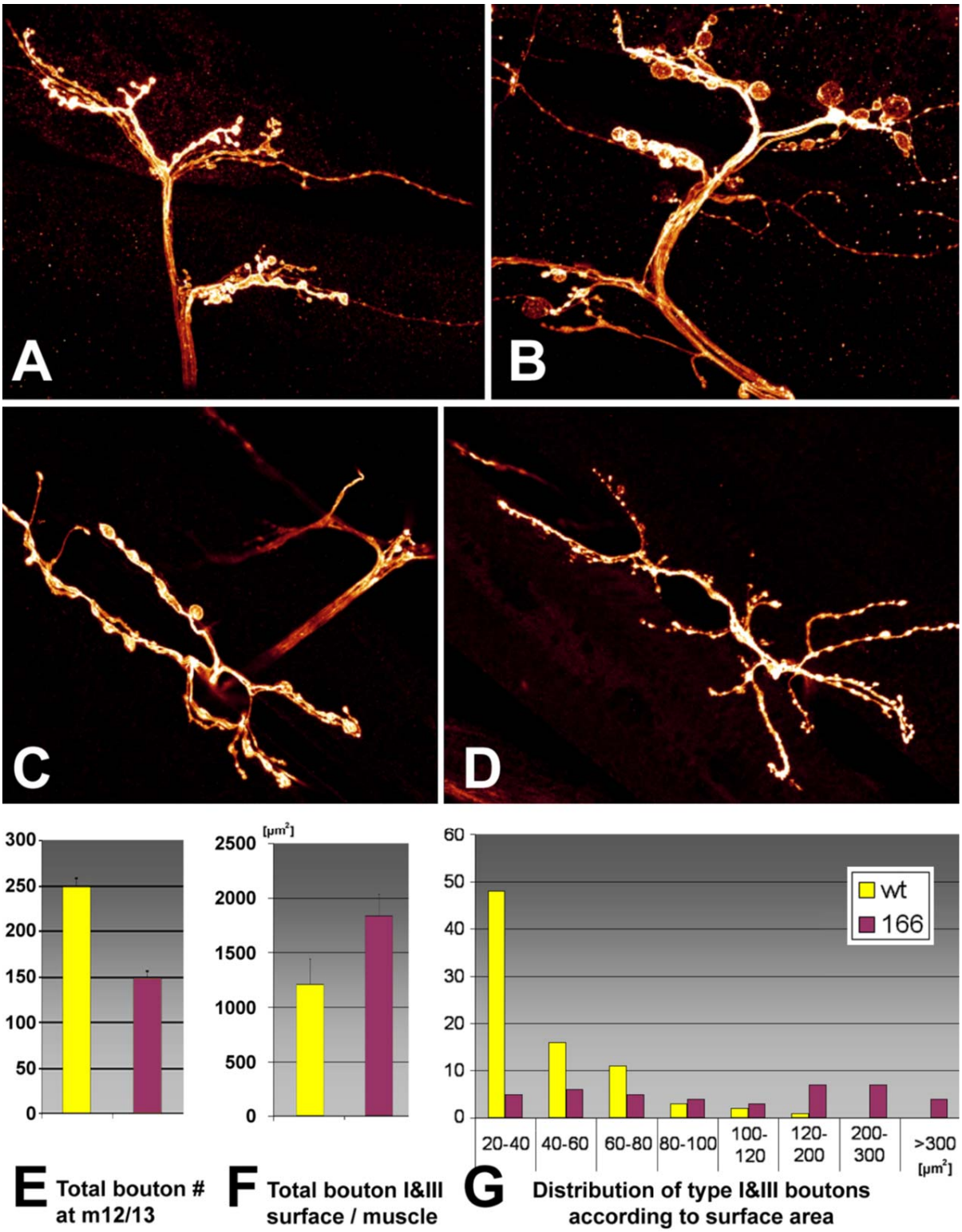

Figure S1. Changes in number and size of boutons at NMJs lacking and overexpressing DVAP-33A. (**A** and **C**) Anti-HRP staining of controls. (**B**) *DVAP-33A*$^{\Delta 166}$ mutant (166) NMJs stained with the same antibodies. (**D**) UAS-DVAP-33A overexpressing NMJs stained with anti-HRP antibodies. (**E**) Quantification of the total number of boutons in control and 166 mutant NMJs. (**F**) Total surface area per muscle for the reported genotypes. (**G**) Calculation of the distribution in synaptic bouton area for the relevant genotypes. A revertant line was used as a control in (A) while in (C) the UAS-DVAP-33A line without the driver was used as a control. *DVAP-33A*$^{\Delta 166}$ mutants exhibit only 150 ± 7 boutons while controls contain 250 ± 8 boutons ($P < 0.001$, n=10 larvae). Similar to null mutations, a decrease in number of boutons and an increase in their size is observed in *DVAP-33A*$^{\Delta 166}$ hypomorphic mutations (see text). The total number of boutons on muscles 12 and 13 was counted. Conversely, neuronal overexpression of *DVAP-33A* induces a dramatic increase in the number of boutons (300 ± 7 versus 180 ± 8, $P < 0.001$, n=12 larvae) with a concomitant decrease in their size (C and D). In this case, the total number of boutons on muscles 6 and 7 was counted.

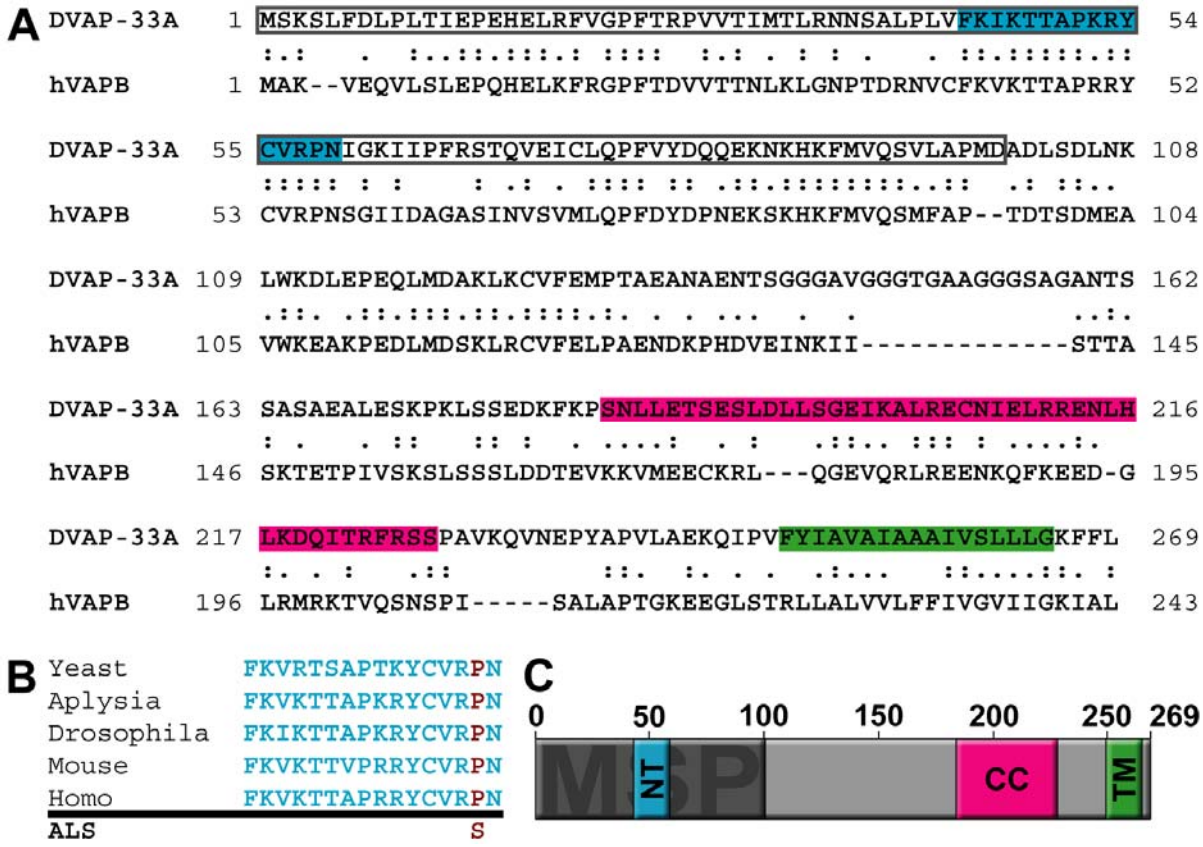

Figure S2. Structural similarity between the human VAPB (hVAPB) protein and its *Drosophila* ortholog DVAP-33A. (**A**) A global protein sequence alignment was performed using the ClustalW v1.82 alignment program available from EMBL-EBI. 93 (39.6%) amino acids were identity matches and 145 (61.7%) were identity matches or conserved substitutions. The sequence for DVAP-33A was taken from FlyBase (Flybase ID FBgn0029687) and the source for the hVAPB sequence was UniProt ID/accession code VAPB_HUMAN/O95292. In the rows between the aligned proteins, ":" represents an identity match, and "." is a conserved substitution according to the GONNET 250 matrix. (**B**) The stretch of 16 amino acids containing the ALS8 mutation changing the Proline 58 into a Serine in DVAP-33A. The alignment shows that this domain is highly conserved in VAP proteins from different species. (**C**) Structure analysis of VAP proteins predicts a trans-membrane domain at the C-terminus (TM) and a coil-coiled domain (CC) in the middle. The grey boxed area corresponds to a domain of significant homology to the nematode Major Sperm Protein (MSP). This region comprises the N-terminal (NT) sequence of 16 amino acids containing the pathogenic mutation. Its function is unknown.

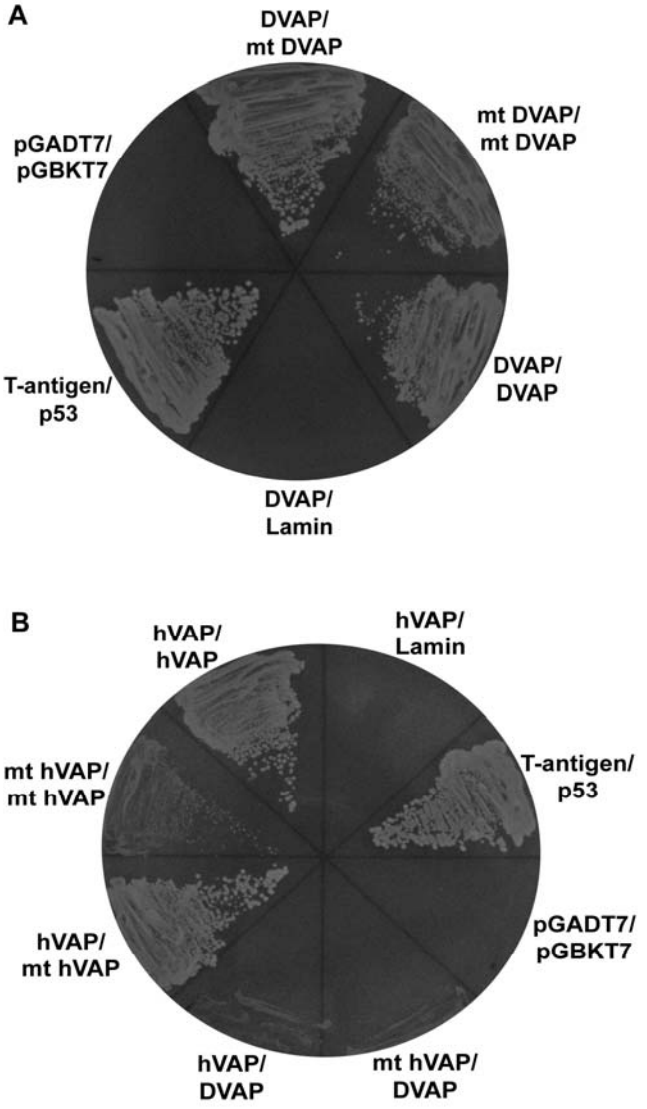

C

	DVAP	mt DVAP
DVAP	+	+
mt DVAP		+

	hVAP	mt hVAP
hVAP	+	+
mt hVAP		+

	hVAP	mt hVAP
DVAP	-	-

Figure S3. Self-oligomerization of wt VAP proteins and mutant VAP proteins detected by yeast two hybrid system. (**A**) Analysis of DVAP-33A (DVAP) and DVAPP58S (mt DVAP) self-oligomerization. (**B**) Homodimerization of hVAPB (hVAP) and hVAPBP56S (mt hVAP); oligomerization of hVAPB with DVAP-33A (hVAP/DVAP) and hVAPBP56S with DVAP-33A (mt hVAP/DVAP). Yeast co-transformed with the indicated constructs in –HALT medium. T-antigen/p53 represents a positive control. pGADT7/pGBKT7 and VAP/lamin represent negative controls. (**C**) Summary of the interactions: "+" represents an interaction, "–" represents no interaction. Black boxes denote interactions reported elsewhere in the table.

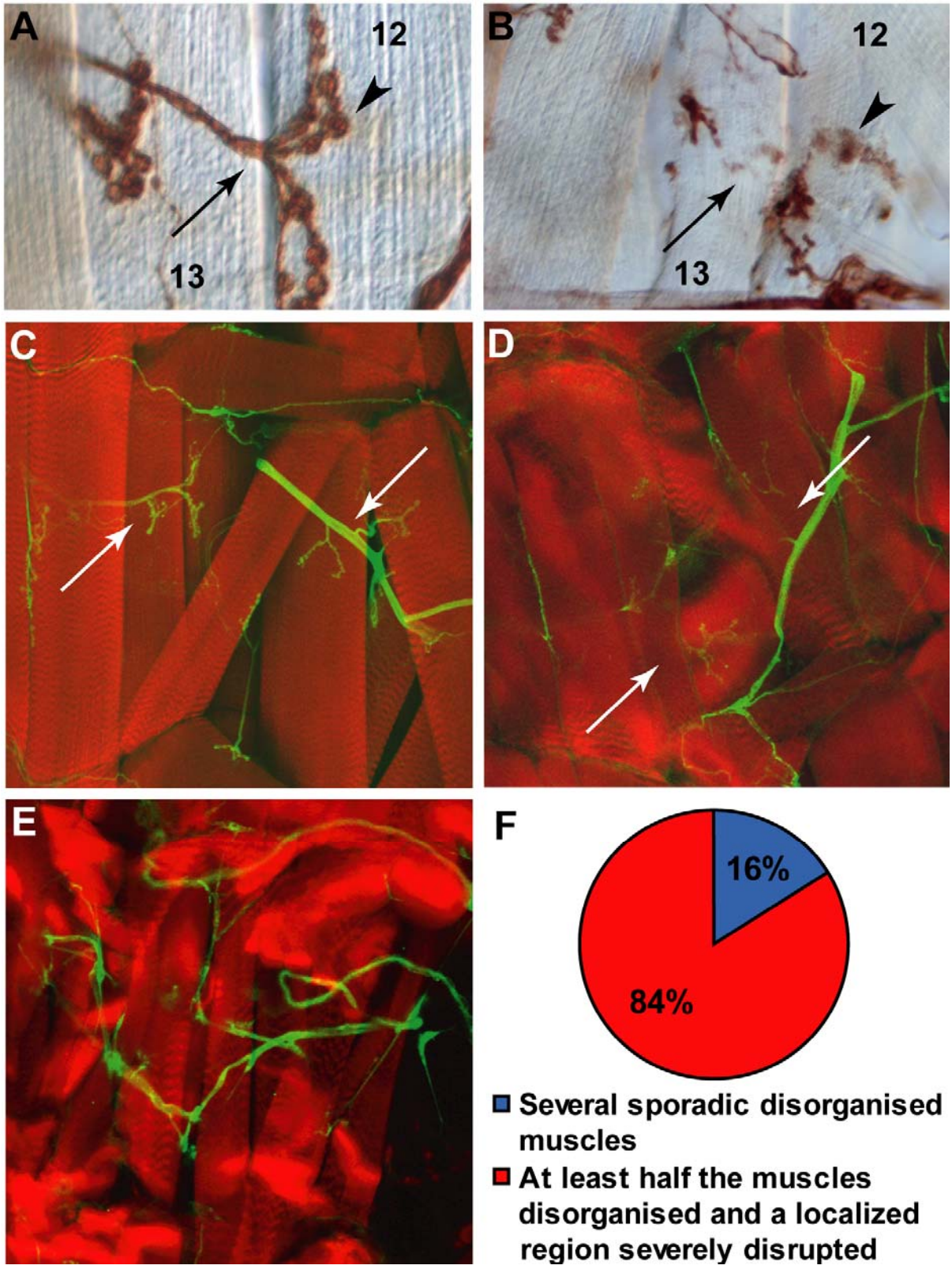
A
12
13
B
12
13
C
D
E
F
16%
84%
Several sporadic disorganised muscles
At least half the muscles disorganised and a localized region severely disrupted

Figure S4. Transgenic expression of DVAPP58S in neurons induces nerve fragmentation and muscle wasting. (**A**) Anti-HRP immunohistochemistry of control NMJs. (**B**) NMJs expressing transgenic DVAPP58S stained with the same antibodies as in (A). (**C**) Anti-HRP immunohistochemistry and phalloidin staining in control synapses. (**D** and **E**) Transgenic DVAPP58S expressing synapses subjected to anti-HRP and phalloidin stainings. (**F**) Quantification of the mutant phenotype. In wt larvae, the motor axon entering the neuromuscular junction is thick and terminal branches contact and sprout on muscle fibers to form a stereotypic arbor (A). Transgenic DVAPP58S expressing synapses exhibit a high range of abnormal morphologies: nerves at the point where they branch onto the muscle fibers are fragmented and the corresponding synapses are not connected to the nerve (compare arrows in C and D). In other cases, the branching nerve is not visible (compare arrows in B and A) and synapses become a highly disorganized, degenerating structure (compare arrowheads in B and A). These synapses contact muscles that exhibit an aberrant morphology when observed by Nomarski optics. The integrity of the muscles at these NMJs was assessed by staining with fluorescence-conjugated phalloidin. In the majority of DVAPP58S transgenic larvae (84%), approximately half of the muscles exhibit an aberrant morphology when compared to controls. Muscles are deformed and slender and exhibit an altered striated pattern (D versus C). In addition, a localized region of severe muscle disruption was observed: muscles become detached from the body wall insertion sites, and muscle loss is accompanied with some remnants of muscle fibers (E)**.** In the remaining 16% of the larvae, sporadic disorganized muscles were observed (F and data not shown). Canton S larvae were used as control in all the experiments reported in this figure. At least 10 larvae per experiment were analyzed.

MATERIALS AND METHODS

Yeast two hybrid interaction

Yeast two-hybrid experiments were performed using the Clontech (Cambridge, UK) Matchmaker system. To analyze the ability of homodimerizing of DVAP-33A and hVAPB as well as of the corresponding protein carrying the ALS8 mutation, the respective cDNAs

were cloned in-frame in pGBKT or in pGAD vectors. Protein interactions were analyzed in media lacking histidine, adenine, leucine and tryptophane (-HALT medium) and containing α-galactosidase following transformation in AH109 yeast strain with the indicated plasmids. In all experiments, pGBKT7-p53/pGADT7-T antigen co-transformation was used as positive control. Negative controls were the co-transformations with the empty vectors pGADT7/pGBKT7 and phVAPB/lamin or pDVAP33A/lamin.